data indicate that PAK does not stimulate MLC phosphatase activity (*30*). Thus, regulation of MLCK activity and, hence, MLC phosphorylation appears to be an important component of Rac- and Cdc42-dependent cytoskeletal remodeling in spreading cells. Because Rho kinase and PAK have opposing effects on MLC phosphorylation, the integrated cellular response to the activation of Rho, Rac, and Cdc42 may depend on the timing of GTPase activation as well as the intracellular localization and extent of MLC phosphorylation.

References and Notes

1. A. K. Wilson *et al.*, *Cancer Metastasis Rev.* **11**, 79 (1992).
2. T. J. Mitchison and L. P. Cramer, *Cell* **84**, 371 (1996).
3. K. Burridge and M. Chrzanowska-Wodnicka, *Annu. Rev. Cell Dev. Biol.* **12**, 463 (1996).
4. C. D. Nobes and A. Hall, *Cell* **81**, 53 (1995).
5. A. Hall, *Science* **279**, 509 (1998).
6. S. Dharmawardhane *et al.*, *J. Cell Biol.* **138**, 1265 (1997).
7. M. A. Sells *et al.*, *Curr. Biol.* **7**, 202 (1997).
8. R. H. Daniels, P. S. Hall, G. M. Bokoch, *EMBO J.* **17**, 754 (1998).
9. R. L. Debiasio *et al.*, *J. Cell Biol.* **107**, 2631 (1988).
10. A. K. Wilson *et al.*, *ibid.* **114**, 277 (1991).
11. J. Howard, *Nature* **389**, 561 (1997).
12. P. de Lanerolle and R. J. Paul, *Am. J. Physiol.* **261**, L1 (1991).
13. A. P. Somlyo and A. V. Somlyo, *Nature* **372**, 231 (1994).
14. R. L. Klemke *et al.*, *J. Cell Biol.* **137**, 481 (1997).
15. P. de Lanerolle, M. Nishikawa, D. A. Yost, R. S. Adelstein, *Science* **223**, 1415 (1984).
16. M. G. Tansey *et al.*, *J. Biol. Chem.* **267**, 12511 (1992).
17. P. de Lanerolle *et al.*, in preparation.
18. Purified smooth muscle MLCK (5.2 μg) was incubated at 30°C for 1 hour by itself (autophosphorylation control) or with constitutively active recombinant glutathione S-transferase–PAK1 (0.5 μg) [U. G. Knaus, S. Morris, H.-J. Dong, J. Chernoff, G. M. Bokoch, *Science* **269**, 221 (1995)] at 30°C in buffer containing 10 mM $MgCl_2$, 2 mM dithiothreitol (DTT), 0.1 mM ^{32}P-labeled adenosine 5′-triphosphate (specific activity ~2000 cpm/pmol), and 20 mM tris-HCl (pH 7.5). Aliquots were removed at various times and analyzed by SDS–polyacrylamide gel electrophoresis (PAGE) and autoradiography. To measure MLCK activity, we incubated autophosphorylated or PAK1-phosphorylated MLCK (50 ng) at room temperature as described above, with 0.5 mM $CaCl_2$, 10^{-7} M calmodulin, 5 mM DTT, and purified regulatory MLC (10 μg). Aliquots were removed at various times and subjected to SDS-PAGE. The bands representing MLC were excised and counted. To quantify changes in MLCK activity in cells, we immunoprecipitated MLCK from nontransfected HeLa cells or from HeLa cells expressing LacZ, wtPAK1, or PAK1 (T423E) as described [P. de Lanerolle, G. Gorgas, X. Li, K. Schluns, *J. Biol. Chem.* **268**, 16883 (1993)] with affinity-purified goat antibodies to MLCK [P. de Lanerolle *et al.*, *Circ. Res.* **68**, 457 (1991)] and protein A–Sepharose. The beads were washed extensively and then assayed for MLCK activity as described. HeLa cells were used in these experiments because the MLCK antibody reacts poorly with BHK-21 MLCK on protein immunoblot analysis.
19. L. S. Price, J. Leng, M. A. Schwartz, G. M. Bokoch, *Mol. Biol. Cell* **9**, 1863 (1998).
20. The cDNAs encoding wtPAK1 or a constitutively active form of PAK1 in which Thr^{423} is mutated into Glu (T423E) were expressed in cells with the Semliki Forest virus Gene Expression System (Life Technologies, Gaithersburg, MD). The cDNAs were amplified using the polymerase chain reaction with primers that contained a Bam HI restriction enzyme site and a Myc tag at the 5′ end. These constructs were subcloned into the Bam HI site of the Semliki Forest vector pSFV3. In vitro transcription of linearized pSFV3 constructs and pSFV-Helper2 was done with SP6 RNA polymerase. RNA transfection of BHK-21 cells was performed by electroporation as described [K. Lundström *et al.*, *Eur. J. Biochem.* **224**, 917 (1994)], yielding recombinant viral stocks of ~10^7 plaque-forming units per milliliter. Viral stocks were stored at −80°C. The virus was activated per manufacturer's instructions, and BHK-21 and HeLa cells were infected in serum-free medium. Transfection efficiency of recombinant virus was routinely >95% in BHK-21 cells and >50% in HeLa cells. Cells were allowed to express protein for 6 to 8 hours after infection in serum-free medium before use in experiments.
21. For cell adhesion assays and immunofluorescence, cells were suspended in basal medium (Glasco minimal essential medium, Life Technologies) containing no serum and seeded in six-well plastic plates containing coverslips coated with fibronectin (20 μg/ml). Cells attached to coverslips were fixed in 4% paraformaldehyde for 20 min, permeabilized with 0.5% Triton X-100 for 20 min, and then incubated with antibody to Myc (9E10) at 1:300 or with antibody to β-galactosidase (β-Gal) at 1:5000 (Promega, Madison, WI) for 1 hour. Cells were then incubated for 1 hour with rhodamine phalloidin 1:500 (Sigma) or with fluorescein isothiocyanate–conjugated antibody to mouse immunoglobulin G (IgG) 1:300 (Cappel Labs, Cochranville, PA) or with both, washed with phosphate-buffered saline, and mounted in Fluoromount-G (Southern Biotechnology Associates, Birmingham, AL). Slides were examined with a Nikon Labophot-ZDFX-DX epifluorescence microscope, and images were photographed with a 35-mm camera and Kodak T-MAX film. For inhibition studies, various concentrations of BDM (Sigma) and ML-7 (Calbiochem, La Jolla, CA) were added to the culture medium.
22. L. P. Cramer and T. J. Mitchison, *J. Cell Biol.* **131**, 179 (1995).
23. Y. Yamakita, S. Yamashiro, F. Matsumura, *ibid.* **124**, 129 (1994).
24. L. C. Sanders and G. M. Bokoch, unpublished data.
25. M. Saitoh, T. Ishikawa, S. Matsushima, M. Naka, H. Hidaka, *J. Biol. Chem.* **262**, 7801 (1997).
26. Cell lysates from control (nontransfected) or transfected BHK-21 cells (35-mm dishes) were separated by SDS-PAGE. Equal volumes (30 μl) were separated on 6 and 15% gels, transferred to polyvinyldifluoride membrane, stained with a 2% Ponceau S solution, rinsed in water, and incubated with milk. The blot from the 6% gel was incubated with an antibody to myosin heavy chain (MHC), whereas the blot from the 15% gel was incubated with an antibody (pp2b) that only recognizes MLC phosphorylated on Ser^{19} [F. Matsumura *et al.*, *J. Cell Biol.* **140**, 119 (1998)]. Protein bands were visualized with horseradish peroxidase–conjugated goat antibody to rabbit IgG (Pierce, Rockford, IL) and with chemiluminescence.
27. M. Chrzanowska-Wodnicka and K. Burridge, *J. Cell Biol.* **133**, 1403 (1996).
28. K. Kimura *et al.*, *Science* **273**, 245 (1996).
29. M. Amano *et al.*, *J. Biol. Chem.* **271**, 29246 (1996).
30. F. Matsumura and G. M. Bokoch, unpublished data.

31. Supported by a U.S. Army Research Breast Cancer Program award to L.C.S. and by grants from the U.S. Public Health Service to F.M., to G.M.B., and to P.d.L. This is publication 11936-IMM from The Scripps Research Institute.

13 October 1998; accepted 26 February 1999

Imaging Protein Kinase Cα Activation in Cells

Tony Ng,[1]* Anthony Squire,[2]* Gurdip Hansra,[1] Frederic Bornancin,[1]† Corinne Prevostel,[1] Andrew Hanby,[3] William Harris,[3] Diana Barnes,[3] Sandra Schmidt,[2] Harry Mellor,[1] Philippe I. H. Bastiaens,[2]‡ Peter J. Parker[1]‡

Spatially resolved fluorescence resonance energy transfer (FRET) measured by fluorescence lifetime imaging microscopy (FLIM), provides a method for tracing the catalytic activity of fluorescently tagged proteins inside live cell cultures and enables determination of the functional state of proteins in fixed cells and tissues. Here, a dynamic marker of protein kinase Cα (PKCα) activation is identified and exploited. Activation of PKCα is detected through the binding of fluorescently tagged phosphorylation site–specific antibodies; the consequent FRET is measured through the donor fluorophore on PKCα by FLIM. This approach enabled the imaging of PKCα activation in live and fixed cultured cells and was also applied to pathological samples.

For many proteins, there is a need to integrate spatial data with information on catalytic function. This is a particular concern in signal transduction processes, where the networking of multiple inputs affects the output, leading to grossly different cellular consequences. Methods applicable to the functional analysis of particular (signaling) proteins in situ would provide a significant advance in reaching a molecular description of cellular behavior.

The classical and novel protein kinase isotypes (cPKC and nPKC, respectively) undergo conformational changes in response to their second messenger, diacylglycerol (DAG) (*1*–*3*). This PKC activator is restricted to membrane compartments, and the stable membrane/DAG-associated complexes formed by PKC have traditionally provided a useful means of monitoring PKC isotype activation (*4*). However, PKC isotypes can associate with mem-

[1]Protein Phosphorylation Laboratory and [2]Cell Biophysics Laboratory, Imperial Cancer Research Fund (ICRF), 44 Lincoln's Inn Fields, London, WC2A 3PX, UK. [3]Hedley Atkins Laboratory, Imperial Cancer Research Fund, Guy's Hospital, St. Thomas Street, London, SE1 9RT, UK.

*These authors contributed equally to this work.
†Present address: Synthelabo Recherche (LERS), 31 Avenue Paul, Valliant-Counturier, 92220 Bagneux, France.
‡To whom correspondence should be addressed. E-mail: (P.I.H.B.) bastiaen@icrf.icnet.uk, and (P.J.P.) parkerp@icrf.icnet.uk

branes before cell stimulation, making membrane association an insufficient criterion for determining PKC activity. We identified a marker of PKCα activation and used FLIM to describe the activation state of PKCα in situ. The utility of this approach is exemplified in analyses of fixed and live cells and additionally of archived human tissues.

PKCα is phosphorylated in vivo on threonine-250 (*5*). A site-specific antiserum to phosphorylated Thr^{250} [T(P)250] reacted with PKCα expressed in COS-7 cells only after treatment of cells with tetradecanoyl phorbol acetate (TPA), and this response was blocked by the PKC inhibitor bisindolylmaleimide I (Fig. 1A). Optimal phosphorylation was induced after 30 min with 400 nM TPA (Fig. 1B). The protein we observed to be T(P)250 immunoreactive is PKCα, as judged by immunoprecipitation and immunoblot (*6*).

Purification of His-tagged PKCα from unstimulated COS-7 cells (*7*), followed by an in vitro autophosphorylation reaction, led to a time-dependent increase in immunoreaction with the T(P)250 antiserum (Fig. 1C). These results demonstrate that the Thr^{250} site is an autophosphorylation site in vitro and in vivo. The equivalent site in PKCβ is also an autophosphorylation site; it is also conserved in PKCγ but not in other PKC isotypes (*6*).

The response of endogenous PKCα was determined in the murine Swiss 3T3 fibroblast line. Exposure of quiescent Swiss 3T3 cells to TPA induced rapid phosphorylation of PKCα (Fig. 1D). This was time-dependent, with optimum phosphorylation induced within 5 min. The dynamics of Thr^{250} dephosphorylation were monitored upon the removal of the relatively hydrophilic agonist, phorbol dibutyrate (PDBu). After a lag period of variable length (10 to 25 min), which probably reflects the reequilibration of cellular PDBu pools, T(P)250 immunoreaction decreased with a half-life of ~5 min (Fig. 1E). Thus, the dynamics of PKC activation can be followed through the immunoreaction of T(P)250.

To monitor the activation of endogenous PKCα, we conjugated the fluorophore Cy3 to

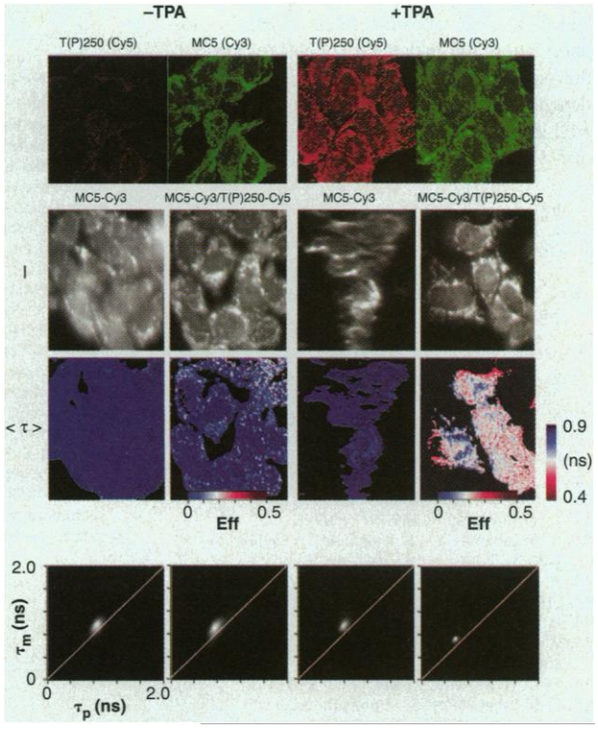

Fig. 2. Endogenous PKCα activation detected by immunofluorescence and FLIM. (Upper panels) Stacked confocal micrographs show an increase in Thr^{250} phosphorylation of endogenous PKCα following 20 min of TPA stimulation (+TPA), as detected by a Cy5-conjugated IgG fraction of T(P)250 [T(P)250-Cy5]. There was no apparent difference in the level of PKCα protein expression before and after TPA treatment, as demonstrated by concomitant detection with MC5-Cy3. Double-label immunofluorescence staining was performed as described (*22*), except for minor modifications (*23*). Antibodies were conjugated to fluorophores as described (*24*). (Middle panels) "I" shows the steady-state fluorescence images from the donor fluorophore (Cy3) conjugated to MC5 in fixed 293T cells, which were stained with either MC5-Cy3 alone or with both MC5-Cy3 and T(P)250-Cy5 (acceptor fluorophore) as indicated (*25*). FRET from the donor (Cy3) to acceptor (Cy5) fluorophore took place on individual PKCα molecules that were phosphorylated after TPA stimulation, resulting in a reduction of the fluorescence emission lifetime of Cy3 as demonstrated by changes in $\langle\tau\rangle$ (the average of τ_p and τ_m). (Lower panels) The 2D histograms quantify the reduction of the donor lifetimes of Cy3 emission for both the phase (τ_p) and modulation (τ_m). A detailed description of the FLIM apparatus used for FRET determination can be found elsewhere (*16*). FRET efficiency color tables (Eff) were calculated from $EFF = 1 - \tau_{da}/\langle\tau_d\rangle$ where τ_{da} is the lifetime map (or color table) of the donor in the presence of acceptor and $\langle\tau_d\rangle$ is the average lifetime of the donor in the absence of acceptor.

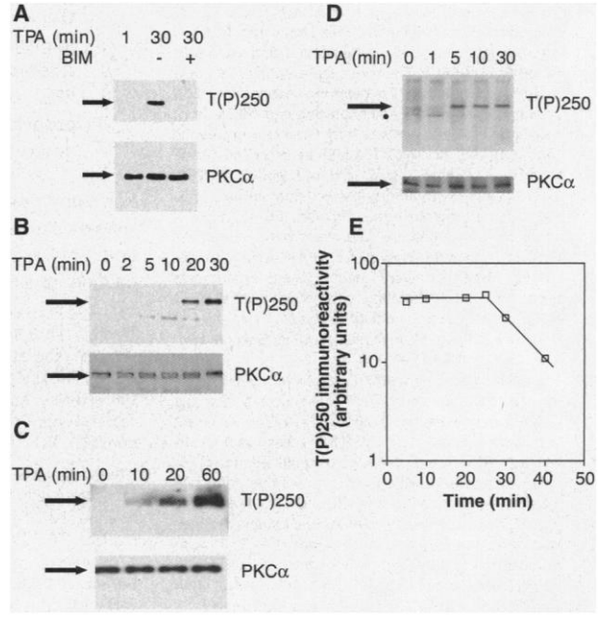

Fig. 1. Identification and detection of an autophosphorylation site on PKCα. (**A**) COS-7 cells were transfected with a cDNA expression plasmid for PKCα. After 48 hours, the cells were treated with TPA for 0 (untreated) or 30 min either in the presence (+) or absence (−) of the PKC inhibitor bisindolylmaleimide I (BIM, 10 μM). The upper panel indicates immunoreactivity with the T(P)250 antiserum (*20*). The lower panel shows immunoreactivity with the MC5 antibody to PKCα protein. (**B**) Transfected COS-7 cells expressing PKCα were treated with TPA (400 nM) for the times indicated. Extracts were prepared and subjected to protein immunoblotting. The upper panel shows the immunoreactivity for the T(P)250 antibody, and the lower panel shows there was no change in PKCα during this treatment. (**C**) COS-7 cell–expressed, histidine-tagged PKCα was purified by nickel-agarose chromatography (*7*). Autophosphorylation of purified PKCα was carried out in the presence of TPA (2 μM), phosphatidylserine (1.25 mg/ml) in 1% (v/v) Triton X-100, 50 mM Hepes (pH 7.5), 12.5 mM $MgCl_2$, and 100 μM ATP. Reactions were initiated with ATP and terminated with Laemmli sample buffer at the times indicated. Phosphorylation of the Thr^{250} site was monitored with the T(P)250 antiserum (upper panel) and the amount of PKCα protein with MC5 (lower panel). (**D**) Quiescent Swiss 3T3 cells (*21*) were treated with TPA for the times indicated. Extracts were prepared and blotted for immunoreaction with the T(P)250 antibody or for PKCα protein. The dot in the upper panel indicates an immunoreactive band that is variably observed and not competed by the phosphopeptide antigen (*6*). (**E**) Quiescent 3T3 cells were treated with PDBu (500 nM) for 20 min, and then washed with medium at 4°C and incubated at 37°C in the absence of PDBu for the times indicated. Cell extracts were blotted with the T(P)250 antiserum, and immunoreaction was quantified by scanning densitometry. The graph illustrates the lag period observed before an exponential decay in T(P)250 immunoreaction.

the MC5 anti-PKCα antibody (MC5-Cy3) and also conjugated the fluorophore Cy5 to purified T(P)250 immunoglobulin G (IgG) [T(P)250-IgG-Cy5]. In unstimulated, fixed 293T cells, heterogeneous staining of the protein was observed with only weak immunoreaction to T(P)250-IgG-Cy5 (Fig. 2, upper panels). Upon stimulation with TPA, T(P)250-IgG-Cy5 immunoreactivity was increased and localized with MC5 immunoreactivity, consistent with activation of PKCα. Colocalization gives only an indication of association, because the determination of proximity is limited by the resolution of the optical system. FRET between Cy3 and Cy5, as measured by FLIM (*8–16*), provides a molecular proximity assay with nanometer-scale resolution for the quantitative determination of the activation and intracellular location of PKCα (*17*). Lifetimes of the Cy3 donor fluorophore (conjugated to MC5) were monitored in cells stained with MC5-Cy3 alone or both MC5-Cy3 and T(P)250-IgG-Cy5. The Cy3 lifetimes (Fig. 2, middle panels) were reduced after stimulation of cells with TPA, when staining was done with both antibodies; for MC5-Cy3 alone, there was no change in lifetimes. The largest reduction in lifetimes (from 1.0 to 0.49 ns) was associated with regions of the plasma membrane and vesicular structures in the cytoplasm. These PKCα-containing vesicular structures overlapped in part with the distribution of ectopically expressed PKCα described for NIH 3T3 cells (*18*). The reduced lifetimes observed in the unstimulated cells were also localized to punctate cytoplasmic structures.

To demonstrate the specificity of the FRET signals as measured by FLIM, cells were stained for PKCα or activated PKCα, or for markers of the endoplasmic reticulum (anti–p62-Cy3) or Golgi (anti–galactosyl transferase-Cy3 or anti–p115-Cy3) (*19*). There was some overlap in localization of PKCα with both compartments; however, there was no FRET between the fluorophores, and thus no reduction in lifetime was observed. The specificity of the PKCα antibody itself (MC5) is essential for the interpretation of the FLIM measurements. After treatment of cells for 18 hours with TPA (1 μM) in order to down-regulate PKCα, immunoreactivity with MC5 was abolished (*19*).

FLIM can be used to analyze a donor-fluorophore–tagged PKCα in live cells microinjected with an excess of acceptor labeled T(P)250-IgG. In transiently transfected COS-7 cells, green fluorescent protein–PKCα (GFP-PKCα) accumulated in a partly cytoplasmic and partly perinuclear location in untreated cells

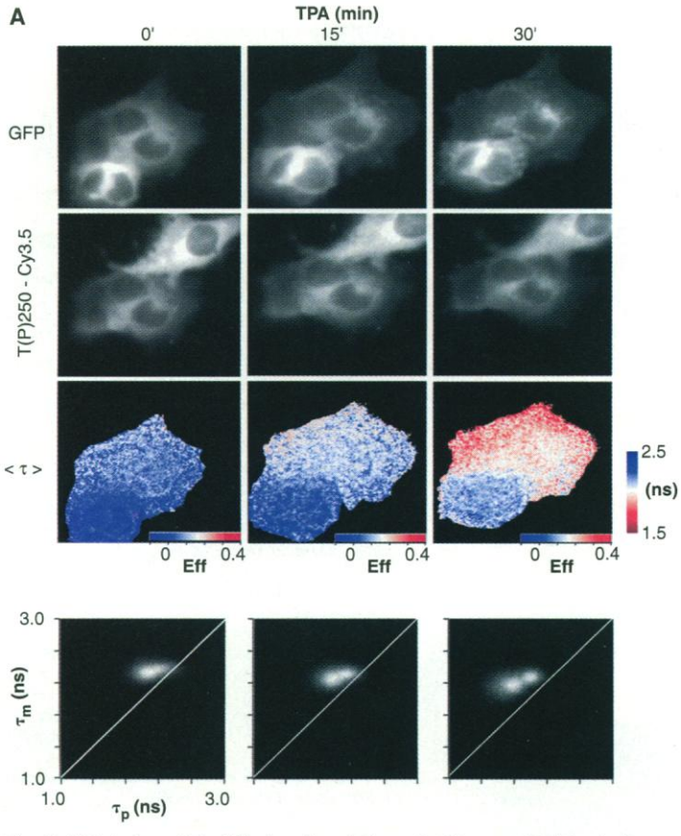

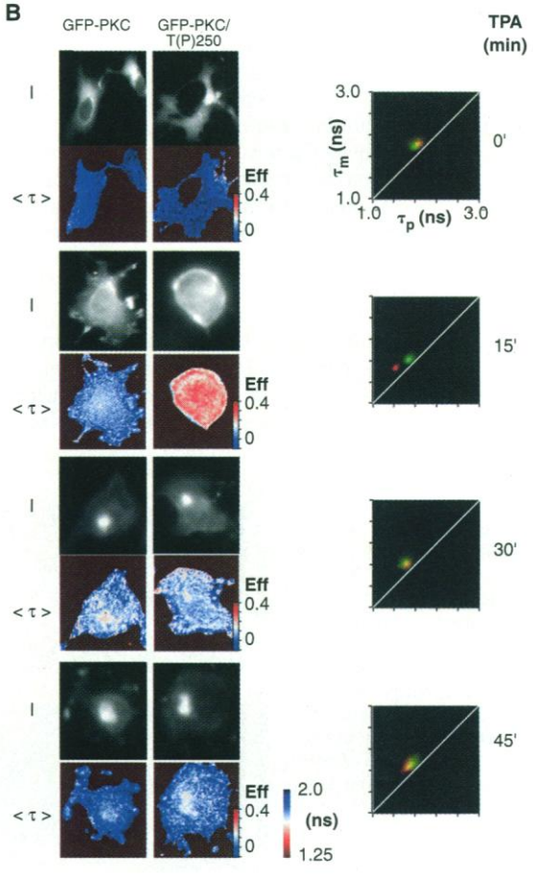

Fig. 3. TPA-induced Thr^{250} phosphorylation of GFP-tagged PKCα in live COS-7 cells detected by FLIM. (**A**) COS-7 cells were transiently transfected with an NH_2-terminal GFP-tagged PKCα construct (details to be described elsewhere) and cultured in serum-containing Dulbecco's modified Eagle's medium for 36 hours before transfer to serum- and phenol red–free Optimax medium (Life Technologies). After an overnight culture, cells were washed and resuspended in phosphate-buffered saline, then microinjected with a Cy3.5-conjugated, protein G–purified IgG fraction of T(P)250. The fluorescence images are shown from the donor (GFP) in four live COS-7 cells which were either left as controls (GFP) or microinjected with T(P)250-IgG-Cy3.5 [T(P)250-Cy3.5]. The bottom four cells were transfected, but only the top three cells (including an untransfected cell) were microinjected with T(P)250-IgG-Cy3.5. By 30 min of TPA stimulation, two separate fluorescence lifetime populations belonging to the microinjected and uninjected cells, respectively, were evident from changes in both the phase (τ_p) and modulation (τ_m) lifetimes of GFP emission (bottom panels). Images shown are representative of five independent experiments. A detailed description of the FLIM apparatus used for FRET determination can be found elsewhere (*16*). (**B**) COS-7 cells were transiently transfected with a GFP-tagged PKCα construct, stimulated with TPA (400 nM), and fixed at various time points as indicated, then either left as controls (GFP-PKC) or stained with T(P)250-IgG-Cy3.5 [GFP-PKC/T(P)250]. The fluorescence images from the donor (I) are shown. The cumulative lifetimes of GFP-PKC alone (green) and that measured in the presence of the acceptor fluorophore [T(P)250-IgG-Cy3.5] (red) are plotted on the same 2D histogram for each time point. For derivation of Eff, see Fig. 2.

(Fig. 3A). After treatment of cells with TPA, there was a progressive increase in GFP-PKCα accumulation in vesicular structures within the cytoplasm; this was most evident after 30 min. The two central GFP-PKCα–transfected cells and one untransfected cell (Fig. 3A) were microinjected with T(P)250-IgG-Cy3.5. The donor fluorophore (GFP), when visualized in the unstimulated cells, was broadly dispersed in the cytoplasm and excluded from the nucleus. Analysis of mean fluorescence lifetime images ($\langle\tau\rangle$, the average of τ_p and τ_m) revealed that there was a small degree of GFP-PKCα phosphorylation in unstimulated cells, but following stimulation, there was a progressive increase in Thr^{250} phosphorylation, evidenced by a decrease in GFP emission lifetimes; this was evident only in the two central GFP-PKCα–transfected and T(P)250-IgG-Cy3.5–microinjected cells. After 15 min, the most intense decrease was observed in punctate areas adjacent to the plasma membrane. By 30 min, there was a greater shift in donor emission lifetimes at the plasma membrane with a broader distribution of shorter lifetimes throughout the cytoplasm. The τ_m and τ_p two-dimensional (2D) histograms show the shift in lifetimes that occurred upon TPA stimulation. Control experiments on fixed cells analyzed by confocal imaging and protein immunoblotting confirmed a redistribution of GFP-PKCα to a perinuclear compartment, but indicated little or no protein degradation within this time frame.

Monitoring of donor emission lifetimes in live cells for up to 40 min after TPA treatment showed that there was a persistent reduction of $\langle\tau\rangle$ in the transfected, microinjected cell population. In contrast, control experiments done in fixed, GFP-PKCα–transfected COS-7 cells revealed a subsequent Thr^{250} dephosphorylation event after approximately 30 min of TPA treatment, with some degree of variation in time course among cells (Fig. 3B). The persistent reduction in $\langle\tau\rangle$ observed in live cells may result from a masking effect of the phospho-specific antibody which protects the epitope from subsequent dephosphorylation by phosphatases that act on PKC. This also shows that the FLIM experiments on live and fixed cells are complementary.

We investigated the activation state of PKCα in fixed tissue samples, using FLIM to provide the required specificity of detection. In a series of formalin-fixed paraffin-embedded breast tumors (n = 23), parallel samples were stained either for PKCα (MC5-Cy3) or for both PKCα and Thr^{250} phosphorylation [T(P)250-IgG-Cy5]. The results obtained fall into two categories: those patients where there was no detectable change in fluorescence lifetime (12 of 23 patients) and those where there was a significant decrease in $\langle\tau\rangle$ (11 of 23) (Fig. 4). Quantification of the τ_p and τ_m changes is provided by the 2D histogram. The results demonstrate that PKCα is activated in situ in a significant number of human breast tumors. Notably, whereas some tumors displayed an up-regulation of PKCα, PKC content per se did not correlate with activation.

The results demonstrate that FRET measured with FLIM is able to detect catalytic functions in vivo as shown by the use of an autophosphorylation site in PKCα to monitor its activation. Our study reveals the dynamics of this phosphorylation process in live cells through donor lifetime properties, revealing the tonic and stimulated juxta-membrane vesicular location of activated PKCα. The studies in fixed cells and tissues complement the analysis and demonstrate the use of these techniques for investigation of human disease.

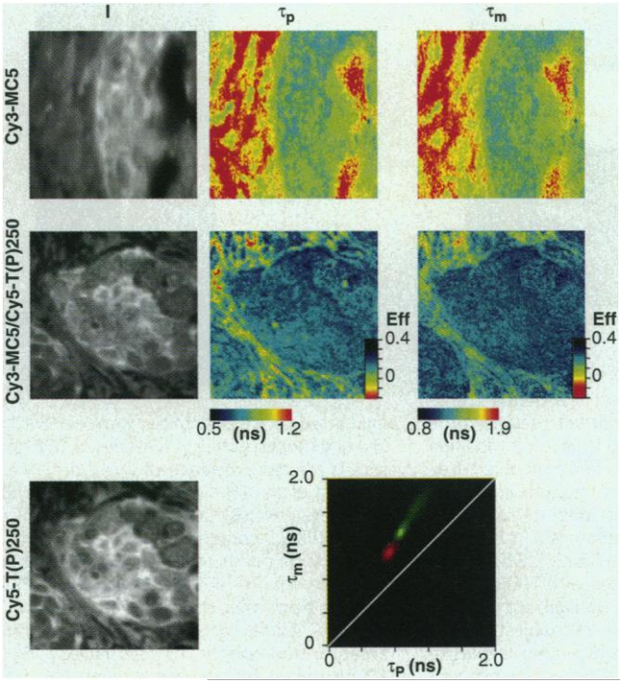

Fig. 4. Demonstration of a variable degree of Thr^{250} phosphorylation of PKCα in paraffin-embedded, fixed tissue sections of human breast carcinomas. Paraffin-embedded breast cancer sections were dewaxed in xylene, pressure cooked for antigen-retrieval (*26*), then stained with either MC5-Cy3 alone or with both MC5-Cy3 and T(P)250-IgG-Cy5. The leftmost panels show the donor (upper and middle) and acceptor (lower) fluorescence patterns. The corresponding lifetime images for the upper two sections are shown at middle and right. The 2D histogram (bottom right) shows the donor lifetimes (τ_p and τ_m) from these images. For derivation of Eff, see Fig. 2.

References and Notes

1. Y. Nishizuka, *Science* **233**, 305 (1986).
2. H. Hug and T. F. Sarre, *Biochem. J.* **291**, 329 (1993).
3. L. V. Dekker and P. J. Parker, *Trends Biochem. Sci.* **19**, 73 (1994).
4. A. S. Kraft and W. B. Anderson, *Nature* **302**, 621 (1983).
5. Thr^{250} was identified following in vivo ^{32}P-labeling of PKCα-transfected COS cells. PKCα was purified from cell extracts, fractionated by SDS–polyacrylamide gel electrophoresis, and digested with trypsin. Labeled peptides were separated by high-performance liquid chromatography and subjected to Edman degradation to identify the phosphorylation sites. One peptide released ^{32}P at cycles 1 and 11, predicting the sites threonine-250 (T250) and serine-260 (S260) derived from an incomplete tryptic cleavage. Confirmation of this identification was derived from the generation of phospho-specific T(P)250 and S(P)260 antisera. Both antisera reacted with PKCα, confirming occupation of these sites. The S260 site is not discussed further here.
6. T. Ng, G. Hansra, P. J. Parker, unpublished data.
7. F. Bornancin and P. Parker, *Curr. Biol.* **6**, 1114 (1996).
8. K. Carlsson and A. Liljeborg, *J. Microsc.* **185**, 37 (1997).
9. C. Y. Dong, P. T. C. So, T. French, E. Gratton, *Biophys. J.* **69**, 2234 (1995).
10. T. W. J. Gadella, R. M. Clegg, T. M. Jovin, *Bioimaging* **2**, 139 (1994).
11. T. W. J. Gadella, T. M. Jovin, R. M. Clegg, *Biophys. Chem.* **48**, 221 (1993).
12. J. R. Lakowicz and K. Berndt, *Rev. Sci. Instrum.* **62**, 1727 (1991).
13. R. Sanders, A. Draaijer, H. C. Gerritsen, P. M. Houpt, Y. K. Levine, *Anal. Biochem.* **227**, 302 (1995).
14. P. C. Schneider and R. M. Clegg, *Rev. Sci. Instrum.* **68**, 4107 (1997).
15. P. T. C. So *et al.*, *Bioimaging* **3**, 1 (1995).
16. A. Squire and P. I. H. Bastiaens, *J. Microsc.* **193**, 36 (1999).
17. Following phosphorylation of PKCα, the molecular proximity of MC5-Cy3 and T(P)250-IgG-Cy5 (that is, when bound to the same PKC molecule) leads to FRET from the donor to acceptor fluorophore and a consequent reduction in the fluorescence lifetime of the donor Cy3 molecule. Only the T(P)250-IgG-Cy5 antibodies that are in close molecular proximity to the MC5-Cy3 are detected through the reduction in fluorescence lifetime of the donor Cy3, whereas all the other acceptor T(P)250-IgG-Cy5 antibodies are not detected in the experiment. Therefore, there is no requirement for absolute specificity of the acceptor fluorophore.
18. J. A. Goodnight, H. Mischak, W. Kolch, J. F. Mushinski, *J. Biol. Chem.* **270**, 9991 (1995).
19. A supplementary figure is available at the *Science* Web site (www.sciencemag.org/feature/data/985808.shl).
20. To obtain antibodies to the two putative phosphorylation sites, the following synthetic phosphopeptides were synthesized in the Peptide Synthesis Laboratory (ICRF, London, UK): GSLS(P)FGVS-amide, WDRT(P)TRND-amide, where the S(P) and T(P) denote the phosphorylated residues S260 and T250 respectively. Phosphopeptides were coupled to keyhole limpet hemocyanin using glutaraldehyde, and the conjugate was employed to immunize rabbits. For protein immunoblotting of immobilized proteins, Tris-buffered saline (pH 7.5) was used in place of phosphate-buffered saline. Antibodies were employed at 1:2000 dilution for 1 hour at room temperature or overnight at 4°C. Immunoreaction was

detected with ECL (Amersham) according to recommended procedures.
21. A. R. Olivier and P. J. Parker, *J. Biol. Chem.* **269**, 2758 (1994).
22. S. C. Kiley, P. D. Adams, P. J. Parker, *Cell Growth Differ.* **8**, 221 (1997).
23. We fixed and permeabilized 293T cells in methanol at −20°C for 4 min. Primary antibodies were diluted 1:200 in 10 mM tris-buffered saline containing 1% bovine serum albumin, except for MC5-Cy3, which was used at 1:50 dilution. The secondary conjugates used were Cy2-conjugated donkey anti-mouse IgG (1:200) and Cy3-conjugated donkey anti-rabbit IgG (1:400) (Jackson ImmunoResearch Laboratories, West Grove, PA). Confocal images were acquired on a confocal laser scanning microscope (model LSM410, Carl Zeiss Inc.) equipped with a ×63/1.4Plan-APOCHROMAT oil immersion objective. Each image represents a 2D projection of sections in the Z series, taken across the depth of the cell at 0.5-μm intervals.
24. P. I. H. Bastiaens and T. M. Jovin, in *Cell Biology: A Laboratory Handbook*, J. E. Celis, Ed. (Academic Press, New York, 1998), pp. 136–146.
25. F. T. Cooke, *et al.*, *Curr. Biol.* **8**, 1219 (1998).
26. C. Gillett *et al.*, *Int. J. Cancer* **69**, 92 (1996).
27. We thank G. Warren and D. Shima (ICRF) for their valuable comments and for antibodies to p62, galactosyl transferase, p115, and giantin. We also thank M. Zerial (European Molecular Biology Laboratory) for a polyclonal antiserum to Rab7. We are grateful to D. Pappin and H. Hansen for protein sequencing.

9 October 1998; accepted 23 February 1999

Regulation of β-Catenin Signaling by the B56 Subunit of Protein Phosphatase 2A

Joni M. Seeling,[1] Jeffrey R. Miller,[3] Rosario Gil,[1]* Randall T. Moon,[3] Ray White,[1] David M. Virshup[1,2]†

Dysregulation of Wnt–β-catenin signaling disrupts axis formation in vertebrate embryos and underlies multiple human malignancies. The adenomatous polyposis coli (APC) protein, axin, and glycogen synthase kinase 3β form a Wnt-regulated signaling complex that mediates the phosphorylation-dependent degradation of β-catenin. A protein phosphatase 2A (PP2A) regulatory subunit, B56, interacted with APC in the yeast two-hybrid system. Expression of B56 reduced the abundance of β-catenin and inhibited transcription of β-catenin target genes in mammalian cells and *Xenopus* embryo explants. The B56-dependent decrease in β-catenin was blocked by oncogenic mutations in β-catenin or APC, and by proteasome inhibitors. B56 may direct PP2A to dephosphorylate specific components of the APC-dependent signaling complex and thereby inhibit Wnt signaling.

In vertebrate cells, Wnt, a secreted glycoprotein, regulates growth and development in part by controlling the activity of a heterodimeric transcription factor containing β-catenin and a member of the Lef-Tcf family of high mobility group transcription factors. β-Catenin binds an APC-axin complex, where it is phosphorylated by glycogen synthase kinase 3β (GSK3β) on NH_2-terminal residues. This phosphorylation event results in the ubiquitin-mediated proteasomal degradation of β-catenin. Wnt signaling leads to the inactivation of GSK3β, which results in an accumulation of β-catenin that then binds to Lef-Tcf and activates transcription of target genes (*1*). Mutations in the APC gene that produce a truncated polypeptide unable to promote the degradation of β-catenin are found in 85% of sporadic colon cancers. Point mutations in β-catenin that alter putative GSK3β phosphorylation sites have been reported in colon, pancreatic, hepatic, and skin cancers (*2*).

[1]Department of Oncological Sciences, Huntsman Cancer Institute, and [2]Department of Pediatrics, University of Utah, Salt Lake City, UT 84132, USA. [3]Howard Hughes Medical Institute, University of Washington, Seattle, WA 98195, USA.

*Present address: Departamento de Bioquimica y Biologia Molecular, Universitat de Valencia, Apartado de Correos 73, 46100 Burjassot (Valencia), Spain.
†To whom correspondence should be addressed. E-mail: david.virshup@hci.utah.edu

The APC protein contains a number of predicted protein-protein interaction domains, suggesting that it acts as a scaffold for the assembly of signaling molecules including β-catenin, GSK3β, and axin. Domains in the central third of APC are required for the binding of these molecules. Armadillo and heptad repeat motifs, which are thought to mediate protein-protein interactions, are present in the NH_2-terminal third of the protein. To identify additional APC-interacting proteins that may regulate Wnt signaling, we performed a two-hybrid screen with the NH_2-terminal third of APC. In a screen of a human B cell cDNA library, clones encoding the B56α and B56δ isoforms of the B56 family of PP2A regulatory subunits were isolated (*3*).

PP2A is an intracellular serine-threonine protein phosphatase. It is a heterotrimeric protein containing conserved catalytic (C) and structural (A) subunits, and a variable regulatory (B) subunit. Three unrelated families of PP2A B subunits have been identified to date, denoted B, PR72, and B56 (B′). These B subunits regulate the subcellular localization and substrate specificity of PP2A, and distinct PP2A heterotrimers can dephosphorylate different sites on the same substrate (*4*). The B56 family of PP2A regulatory subunits includes five widely expressed paralogous genes (α, β, δ, ε, and γ) (*5*, *6*). To confirm the interaction of APC and B56, we tested plasmids encoding a number of PP2A subunits for interaction with APC in a directed two-hybrid assay (*7*). APC interacted with all assayed members of the B56 family, whereas there was no detectable interaction with Bα (a member of the B family), PR72, A, or C subunits (*8*).

One essential function of the Wnt pathway signaling complex is to regulate the abundance of β-catenin. Multiple phosphorylation events occur in this complex, including the phosphorylation of APC, GSK3β, β-catenin, and axin (*9*). The possible interaction of a PP2A regulatory subunit with this complex indicates that phosphatase activity may regulate β-catenin signaling. To test this, we assessed the effect of okadaic acid, a cell-permeable serine-threonine phosphatase inhibitor, on β-catenin abundance. Treatment of HEK 293 cells with okadaic acid caused an increase in the abundance of β-catenin (Fig. 1A). This suggests that if a PP2A heterotrimer participates in the Wnt–β-catenin pathway, it is likely to be inhibitory to the signaling process. We therefore determined whether increased expression of B56 had any effect on the amounts of β-catenin in 293 cells. Expression of B56α decreased the amount of β-catenin (Fig. 1B). Expression of other members of the B56 family also reduced the abundance of β-catenin (Fig. 1C). The down-regulation of β-catenin was specific to the B56 family, however, because transfection of empty vector, or expression of Bα, had no effect on the amount of β-catenin.

The degradation of phosphorylated β-catenin can be blocked by proteasome inhibitors (*10*). We therefore transfected 293 cells with vectors encoding hemagglutinin (HA)-tagged B56α and either Myc-tagged β-catenin (Fig. 2A) or untagged β-catenin (Fig. 2B) and then treated the transfected cells with the proteasome inhibitors MG-132 (Fig. 2A) or *N*-acetyl-Leu-Leu-norleucinal (ALLN) (Fig. 2B). In both instances, the B56-induced decrease in β-catenin abundance was blocked by the inclusion of the proteasome inhibitor. The peptide aldehyde calpain inhibitor *N*-acetyl-Leu-Leu-methional (ALLM) had no effect on the B56-induced degradation of β-catenin (*8*).

Deletion of the first 90 amino acids of β-catenin (Δ90β-catenin) that encompass the putative GSK3β phosphorylation sites produces a stable protein that accumulates in the